

Heavy-fermion valence-bond liquids in ultracold atoms: Cooperation of Kondo effect and geometric frustration

L. Isaev and A. M. Rey

JILA, NIST & Department of Physics, University of Colorado, 440 UCB, Boulder, CO 80309, USA

We analyze a microscopic mechanism behind coexistence of a heavy Fermi liquid and geometric frustration in Kondo lattices. We consider a geometrically frustrated periodic Anderson model and demonstrate how orbital fluctuations lead to a Kondo-screened phase in the limit of extreme strong frustration when only local *singlet* states participate in the low-energy physics. We also propose a setup to realize and study this exotic state with $SU(3)$ -symmetric alkaline-earth cold atoms.

PACS numbers: 71.27.+a, 75.10.Kt, 67.85.-d, 37.10.Jk

Introduction. Geometric lattice frustration plays a crucial role in Mott insulators [1] where it usually suppresses long-range magnetism by enhancing the number of competing magnetic ground states. At zero temperature, this degeneracy may be relieved in favor of a quantum non-magnetic phase such as a spin liquid or valence bond ordering [2]. On the contrary, lattice topology in most metals is less important due to long-range magnetic interactions mediated by the itinerant electrons and small static magnetic moments.

The situation is different in cases when magnetic and itinerant behaviors originate from physically distinct degrees of freedom [3]. For example, in heavy-fermion (HF) metals [4, 5] magnetic moments arise from localized $4f$ or $5f$ -electrons, while conduction electrons typically reside in extended atomic s -orbitals. Low-temperature properties of such systems are driven by several opposing quantum many-body effects: (i) Kondo screening, i.e. formation of singlets between local moments and itinerant electrons that gives rise to “heavy” quasiparticle states with delocalized f -electrons; (ii) local-moment long-range magnetism; and (iii) non-magnetic states due to lattice frustration that involve singlets only among local spins. Geometrically frustrated f -electron compounds [or Kondo lattices (KLs)] such as $\text{Yb}_2\text{Pt}_2\text{Pb}$ [6] received much attention in the recent years [7–10].

The magnetism, Kondo effect, and geometric frustration compete because they involve same local electrons which can not simultaneously form singlets with each other and the conduction band. This observation is at the heart of the recently proposed generic phase diagram of HF materials [7] that allows their classification according to the amount of quantum fluctuations of local magnetism [11]. Naturally, this phase diagram precludes Kondo screening in strongly-frustrated lattices. The antagonism between Kondo effect and lattice frustration only occurs in cases that involve pure spin degrees of freedom. In contrast, in systems with multiple local orbitals, orbital fluctuations allow local *spin singlets* to participate in the Kondo screening [12, 13] together with the usual “spinful” states. If the singlets were due to frustration, the local orbital fluctuations might provide a pathway

towards a strongly-frustrated Kondo-screened state.

In the present Letter we argue that such phase with coexisting Kondo and frustration-driven local-spin singlets can indeed be realized. To demonstrate this, we consider a toy system – a periodic Anderson model on a triangular tube lattice (TTL) of Fig. 1(a) with frustrated triangular plaquettes (due to large antiferromagnetic exchange interaction between localized electrons) in the Kondo regime when valence fluctuations are suppressed and each plaquette has a spin-singlet ground state (GS) with exactly two fermions. Because of different possible arrangements of local *valence bond* (VB) singlets [14], this GS is *triply degenerate*. Although local spins are quenched in the singlet states, orbital fluctuations [Fig. 1(b)] allow mixing of the VB configurations by the Anderson hybridization with the conduction band, and give rise to a robust Kondo-screened GS with heavy quasiparticles and delocalized VB singlets [Fig. 1(c)].

This KL can be implemented using fermionic alkaline-earth atoms (AEAs), i.e. atoms with two outer electrons, in an optical lattice [see Fig. 1(d)]. AEAs prepared in the two lowest clock states (1S_0 and 3P_0) with total angular momentum $J = 0$ show a strict decoupling of electronic orbital and nuclear-spin degrees of freedom, and obey an accurate $SU(N \leq 2I + 1)$ (I is the nuclear spin) symmetry in the two-body collisions [15] which has been recently verified with ^{87}Sr [16] and ^{173}Yb [17, 18]. Our key observation is that the local VB singlets can be encoded with entangled states of two AEAs [Fig. 1(e)] prepared in different clock configurations and three nuclear spin levels. The degeneracy of these states is *guaranteed by the* $SU(N = 3)$ *symmetry*. The entangled atomic pairs are loaded in the lowest, strongly localized, band of a *magic* optical lattice whose trapping potential does not affect clock transitions [19], and *implement the locally frustrated plaquettes* (the optical lattice itself does not need to be geometrically frustrated). The conduction electrons are simulated by placing AEAs in a higher, itinerant band.

At low energies, both of the above systems are described by a KL model with a peculiar $SU(3)$ structure. In the metallic regime, its GS is a Fermi [in one dimension (1D), Luttinger] liquid consisting of delocalized VB

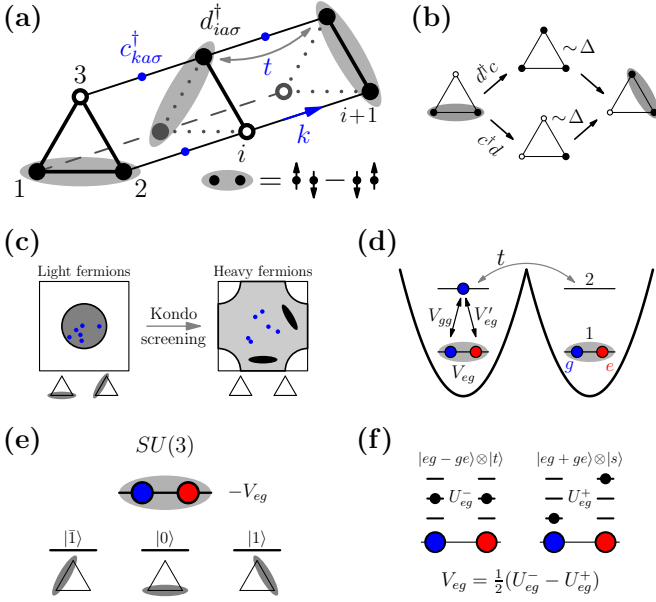


FIG. 1. Panel (a) the triangular tube lattice. Black and blue circles denote local ($d_{ia\sigma}^\dagger$) and itinerant ($c_{ka\sigma}^\dagger$) electrons. Grey ellipses are VB singlets (2) (empty circles indicate holes). Itinerant fermions propagate (by hopping between triangles with an amplitude t) in the leads with momentum k . (b) Valence fluctuations away from the two-electron singlet GS of a triangle, leading to VB flips. (c) Schematic plot of delocalization of the VB singlets and heavy-quasiparticle formation due to the Kondo screening. Shaded regions are Fermi surfaces in the Brillouin zone. (d) Magic optical lattice that implements the frustrated KL model (3) [band 1 (2) is localized (itinerant)]. Red and blue circles are AEAs in 3P_0 (e) and 1S_0 (g) clock states. Grey ellipses show local e - g entangled states (with energy $-V_{eg}$). V'_{eg} and V_{gg} are the inter-band exchange interactions ($V_{eg} \gg V'_{eg}, |V_{gg}|$). (e) Mapping from VB singlets on a triangle to lowest-energy e - g pair states for $SU(3)$ AEAs. (f) Two different scattering lengths for spin symmetric $|t\rangle$ and antisymmetric $|s\rangle$ channels. The three levels indicate nuclear spin states for each atom (black circle marks a populated state).

singlets (AEA pairs) screened by itinerant fermions, that can be viewed as a short-range resonant VB spin liquid [20] *stabilized by the Kondo effect*.

Toy model: $SU(3)$ KL on a TTL. Let us consider a periodic Anderson model on the lattice of Fig. 1(a):

$$H^{TTL} = \sum_{ka\sigma} \varepsilon_{k\sigma} c_{ka\sigma}^\dagger c_{ka\sigma} + v \sum_{ia\sigma} (c_{ia\sigma}^\dagger d_{ia\sigma} + \text{h.c.}) + \quad (1)$$

$$+ \sum_i \left[J_H \mathbf{S}_d^2(x_i) - \varepsilon_d N_d(x_i) + U \sum_{a \neq b} n_{ia}^d n_{ib}^d \right] + H_{\text{mix}},$$

which describes a system of conduction electrons $c_{ka\sigma}$ with momentum k in the a th lead ($a = 1 \dots 3$), spin $\sigma = \{\uparrow, \downarrow\}$, hybridized (via an amplitude v) with local electrons $d_{ia\sigma}$ at each vertex a of a triangle at position $x_i = i$. $N_d = \sum_a n_{ia}^d = \sum_{a\sigma} d_{ia\sigma}^\dagger d_{ia\sigma}$ and

$S_d = \frac{1}{2} \sum_{\alpha\beta} d_{ia\alpha}^\dagger \sigma_{\alpha\beta} d_{ia\beta}$ (σ are Pauli matrices) define electron number and total spin of a triangle. The dispersion $\varepsilon_{k\sigma} = \varepsilon_k - h\sigma$ includes a small (compared to other magnetic interactions) Zeeman splitting h whose role we explain later. The term H_{mix} describes mixing of fermions in different leads a and for now will be ignored.

There are several energy scales associated with each triangle: local binding energy $\varepsilon_d > 0$, the nearest-neighbor Coulomb repulsion U , ‘‘Hund’’ energy $J_H \geq 0$ that forces the lowest total spin S_d , and an infinitely large on-site Coulomb repulsion preventing double occupancy of any vertex a . We focus on a two-electron $S_d = 0$ subspace which contains a three-fold degenerate GS when $U - \frac{3}{4}J_H < \varepsilon_d < 2U + \frac{3}{4}J_H$:

$$|a\rangle_i = \frac{1}{\sqrt{2}} \sum_{b'b} s_{b'b}^a d_{ib'\uparrow}^\dagger d_{ib\downarrow}^\dagger |\text{vac}\rangle, \quad (2)$$

where $s_{b'b}^a = s_{bb'}^a = 1$ when a, b and b' are different, and 0 otherwise; $|\text{vac}\rangle$ is the vacuum ($N_d = 0$) state. These states are labeled by the number of an unoccupied vertex.

We will fix $\varepsilon_d = \frac{3}{2}U$ and consider the strong-coupling regime $v \ll \varepsilon_d, U, J_H$ when N_d -fluctuations on each triangle are virtual and can be taken into account via a generalized Schrieffer-Wolff transformation \mathcal{S} [21] that includes processes shown in Fig. 1(b). A straightforward calculation yields the second-order KL Hamiltonian

$$H_{\text{ef}}^{TTL} = \sum_{ka\sigma} \varepsilon_{k\sigma} c_{ka\sigma}^\dagger c_{ka\sigma} - \sum_{iab} V_{ab} f_{ia}^\dagger f_{ib} c_{ia\sigma}^\dagger c_{ib\sigma} \quad (3)$$

that describes scattering of conduction electrons by the local VB singlets and is defined on a *non-frustrated* lattice whose sites correspond to triangles in Fig. 1(a). The coupling constants are $V_{ab} = V_\perp(1 - \delta_{ab}) + V_\parallel \delta_{ab}$ with $V_\perp = -\frac{v^2}{2\Delta}$, $V_\parallel = \frac{3v^2}{2\Delta}$, δ_{ab} – the Kronecker delta, and the valence fluctuation gap $\Delta = \frac{1}{2}U + \frac{3}{4}J_H$. The states (2) are described with a pseudo-fermion representation [5]:

$$|a\rangle_i \rightarrow f_{ia}^\dagger |\text{vac}\rangle \quad (4)$$

with a Hilbert space constraint $\sum_a f_{ia}^\dagger f_{ia} = 1$. Because only $S_d = 0$ triangle states are involved in the low-energy physics, interactions in H_{ef}^{TTL} preserve electron spin σ and only change the orbital (lead) degree of freedom a .

As a result, Eq. (3) describes a two-channel KL model (spin is the channel index) [22]. It is known that the two-channel fixed point is usually unstable w.r.t. channel asymmetry [22] controlled by the Zeeman splitting h . Since even for small $h \ll J_H$ the leads may be considered spin-polarized, below we omit the spin index σ and replace $c_{ia\sigma} \rightarrow c_{ia\uparrow} \equiv c_{ia}$ and $\varepsilon_{k\sigma} = \varepsilon_{k\uparrow} \approx \varepsilon_k$.

The Hamiltonian (3) contains matrix elements connecting all three possible local VB states and conduction electron ‘‘flavors’’ a , and is an anisotropic (XXZ -like) $SU(3)$ KL model written in terms of generators $T_a^b(x_i) = f_{ia}^\dagger f_{ib}$ and $\tilde{\tau}_a^b(x_i) = c_{ib}^\dagger c_{ia}$ for local and itinerant degrees of freedom [23]. The local $SU(3)$ ‘‘spin’’

operators $T_a^b(x_i)$ describe orbital fluctuations in Eq. (1) that flip the VB singlets (2). H_{ef}^{TTL} in Eq. (3) is invariant under $U(1)$ transformations $f_{ia} \rightarrow e^{i\phi_a} f_{ia}$ and $c_{ia} \rightarrow e^{-i\phi_a} c_{ia}$ that preserve the V_{\perp} term. There is also a discrete lattice symmetry $C_{3v} = \{C_3, \sigma_v\}$ [24] that contains $\frac{2\pi}{3}$ (C_3) rotations around the TTL axis and three symmetry planes σ_v of the triangles.

Kondo effect-assisted VB phases. To demonstrate that the model (3) has a Kondo screened GS, we use a generalized hybridization mean-field (HMF) approach [25] that treats the f -fermion Hilbert space constraint on average, $\frac{1}{N} \sum_{ia} \langle f_{ia}^{\dagger} f_{ia} \rangle = 1$ (N is the system size), and self-consistently compute the hybridization and $SU(3)$ “magnetization” order parameters (OPs) [26]. We assume that all OPs are site-independent. There are three hybridization amplitudes: $\chi_0 = \frac{1}{\sqrt{3}} \sum_a \langle f_{ia} c_{ia} \rangle$, $\chi_{1,2} = \frac{1}{\sqrt{3}} \langle f_{i1} c_{i1} + \omega^{\mp 1} f_{i2} c_{i2} + \omega^{\pm 1} f_{i3} c_{i3} \rangle$ with $\omega = e^{2\pi i/3}$, and eight magnetizations m_l^c [m_l^f] for c - [f -] fermions defined via $\langle c_{ia}^{\dagger} c_{ib} \rangle = \sum_l \lambda_{ab}^l m_l^c + \frac{n^c}{3} \delta_{ab}$ [$\langle f_{ia}^{\dagger} f_{ib} \rangle = \sum_l \lambda_{ab}^l m_l^f + \frac{1}{3} \delta_{ab}$] where λ^l are the Gell-Mann matrices, $l = 1 \dots 8$ and n^c is the conduction band filling. Unlike the real $SU(2)$ magnetization, $m^{c,f}$ do not break time-reversal invariance but rather the above $U(1)$ and C_{3v} symmetries. The OPs χ_1 and χ_2 are connected (up to a phase) by the planes σ_v from C_{3v} . Finite $m_{3,8}^{c,f}$ completely break C_{3v} leading to nematic states; $m_l^{c,f}$ with $l \neq 3, 8$

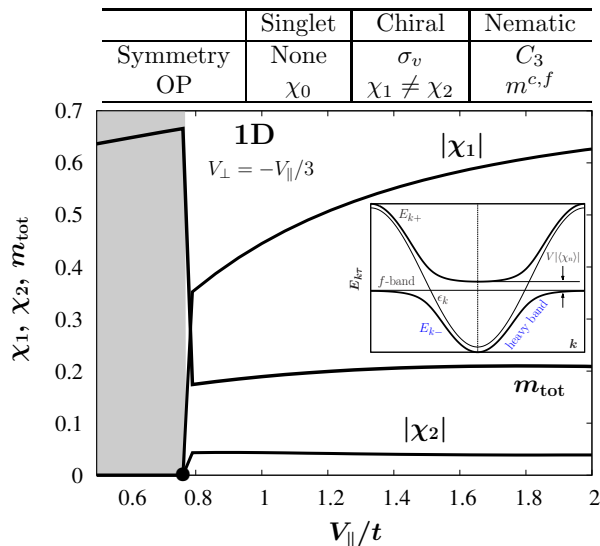


FIG. 2. $T = 0$ phase diagram of the KL model (3) with $N = 4900$ sites and electron density $n^c = 0.8$. $m_{\text{tot}} = [(m_3^c + m_8^f)^2 + (m_5^c + m_6^f)^2]^{1/2}$ plays a role of the total magnetization. The black circle at $V_{\parallel}/t \sim 0.76$ marks the first order transition between Kondo-screened and normal phases. Inset: The HF band-structure. The band splitting at the Fermi level is $\sim V\chi_{1,2}$. The table shows symmetries broken by different OPs and corresponding VB liquid phases.

also break the above $U(1)$ symmetry.

Kondo-screened states correspond to nonzero values of either hybridization OP $\chi_{0,1,2}$. In analogy to spin systems [27, 28], we call phases with $\chi_1 \neq \chi_2$ chiral [29]. This discussion is summarized in the table in Fig. 2.

The phase diagram of the Hamiltonian (3) is shown in Fig. 2 for $\epsilon_k = -2t \cos k$ (t is the nearest-neighbor hopping). There is a first order transition between a normal state with $\chi_{0,1,2} = 0$, and a Kondo screened phase with $\chi_1 \neq \chi_2 \neq 0$ (but $\chi_0 = 0$) and non-zero $m_{3,8}^{c,f}$. This chiral nematic phase has delocalized VB singlets. The OPs $m^{c,f}$ survive only at low temperature $T \leq T_c \sim 5 \times 10^{-2}t$; for $T > T_c$ the only finite OP is χ_1 and the GS realizes a chiral metallic VB spin liquid.

This phase is quite different from the Kondo-stabilized spin liquid of Ref. 30 where the resonating VBs of local spins are formed due to their coupling to conduction band and are unstable away from the Kondo regime. In our case the VB singlets are due to geometric frustration, and the Kondo screening only injects them into the Fermi sea.

Stability of the Kondo-assisted VB liquid. The Kondo phase in Fig. 2 is quite robust against changes in the noninteracting itinerant density of states (DOS). To show this, we consider a model DOS that corresponds to a square lattice with nearest-neighbor hopping $\epsilon_k = -2t(\cos k_x + \cos k_y)$ (as opposed to the 1D tight-binding dispersion used before), see inset in Fig. 3. The phase diagram obtained by applying the HMF approach to the KL (3) is presented in Fig. 3. Unlike the 1D case in Fig. 2, the chiral VB liquid with $\chi_1 \neq 0$, $\chi_{0,2} = 0$ and $m^c = m^f = 0$ exists even at $T = 0$ for $V_{\perp} \leq 0$ and large V_{\parallel} . Only mirror symmetry from C_{3v} is broken by this state. With decreasing $|V_{\perp}|$ and V_{\parallel} the system undergoes a transition to a nematic metallic state with $m^{c,f} \neq 0$ and completely broken C_{3v} . The situation is different for $V_{\perp} \geq 0$. Here the only non-zero OP is χ_0 and the VB liquid GS does not break any discrete symmetry. All these Kondo-screened states become unstable at small $|V_{\perp}|$ and V_{\parallel} .

The phase transitions in Fig. 2 and 3 are first order which may be an artifact of the HMF approximation. In general at $T = 0$ the emergence of nonzero OPs $\chi_{0,1,2}$ is associated with a *phase transition* (as opposed to a crossover) when fluctuations beyond HMF are taken into account [31]. Therefore salient features of our phase diagrams should remain unchanged.

Finally, we mention effects of a finite lead-mixing H_{mix} in Eq. (1). Its simplest form (compatible with C_{3v} symmetry of the TTL) corresponds to hopping of itinerant and local fermions around the triangle. This correction results [32] in a Zeeman-like term, proportional to the intra-triangle hopping, which lifts degeneracy of the local VB states (2) and can suppress the Kondo phase in Fig. 2 if this splitting is sufficiently large [4].

Implementation with ultracold AEs. We propose an experimentally accessible implementation of the KL

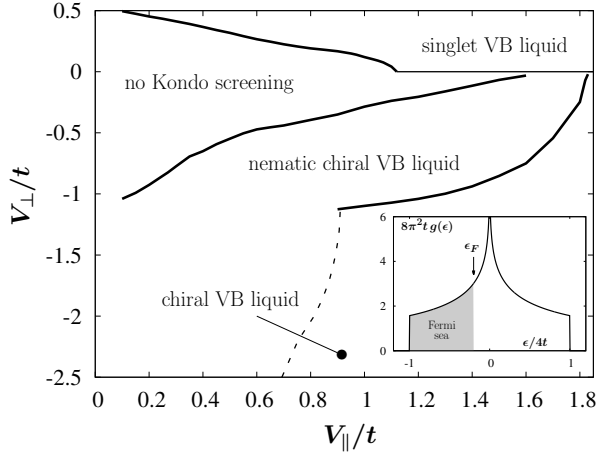


FIG. 3. Generic $T = 0$ phase diagram of Eq. (3) [or (7) with $U_{gg} = 0$] with $N = 3600$ sites and $n^c = 0.8$. All phase transitions are first order. Inside the nematic phase there is a “metamagnetic” transition between states with $m_1^{c,f} \neq 0$, $m_{3,8}^{c,f} = 0$ (at smaller V_{\parallel}) and $m_1^{c,f} = 0$, $m_{3,8}^{c,f} \neq 0$ (for larger V_{\parallel}) which are separated by a continuation of the dashed line. Inset: Noninteracting itinerant DOS $g(\epsilon) = \frac{1}{8\pi^2 t} K(\sqrt{1 - (\epsilon/4t)^2})$ [$K(x)$ is elliptic integral of the 1st kind] used to compute the phase diagram.

model (3) with AEAs in an optical lattice, *that is free of the mixing* described by H_{mix} . The key idea of our approach is to use nuclear spin states of the atoms as “synthetic” frustrated plaquettes [corresponding to triangles in Fig. 1(a)] and construct an appropriate low-energy model that takes into account these local states as well as the itinerant degrees of freedom, and is unitarily related to the KL model (3). The GS degeneracy of a synthetic plaquette is guaranteed by the $SU(N = 3)$ symmetry of the AEAs.

Consider a two-band optical lattice schematically shown in Fig. 1(d). The lowest-energy band is localized and contains two AEAs per site in different clock states: one 1S_0 (GS, g) and one 3P_0 (excited state, e). To minimize lossy e - e collisions, the higher-energy itinerant band is populated only by g atoms. The Hamiltonian of the system is [15]:

$$H^A = -t \sum_{\langle ij \rangle} (c_{in}^\dagger c_{jn} + \text{h.c.}) + \sum_i \left[\frac{U_{gg}}{2} n_i^c (n_i^c - 1) + \right. \\ \left. + (V_{gg} g_{in}^\dagger g_{im} + V'_{eg} e_{in}^\dagger e_{im}) c_{im}^\dagger c_{in} + V_{eg} e_{in}^\dagger e_{im} g_{im}^\dagger g_{in} \right],$$

where g_{in} (e_{in}) denote g (e) fermions in the localized band at site i and nuclear spin state $n = \bar{1}, 0, 1$ [$\bar{n} = -n$, i.e. $\bar{1} = -1$, $\bar{0} = 0$], and c_{in}^\dagger create itinerant g atoms. There is an implicit summation over nuclear spin indices. The first term describes nearest-neighbor hopping with an amplitude t . The second sum corresponds to e - g (V_{eg} and V'_{eg}) and g - g (V_{gg}) exchange couplings, as well as

direct g - g interaction $U_{gg} \geq 0$ [see Fig. 1(d)-(f)]. V_{eg} and V'_{eg} have the same sign, and V_{gg} is negative [33].

States of a localized e - g pair are described by the term $H_{\text{loc}}(x_i) = V_{eg} g_{in}^\dagger g_{im} e_{im}^\dagger e_{in}$ whose spectrum consists of a triply-degenerate GS subspace with energy $-V_{eg}$:

$$|l\rangle_i = \frac{1}{\sqrt{2}} \varepsilon_{lnm} e_{in}^\dagger g_{im}^\dagger |\text{vac}\rangle \quad (6)$$

(ε_{lnm} is the antisymmetric Levi-Civita tensor, $\varepsilon_{10\bar{1}} = 1$), and a sextet $|l\rangle'_i = (1/\sqrt{2}) s_{nm}^l e_{in}^\dagger g_{im}^\dagger |\text{vac}\rangle$ [s_{bc}^a was defined in (2)] and $|l\rangle''_i = e_{il}^\dagger g_{il}^\dagger |\text{vac}\rangle$ with energy $+V_{eg}$. We assume that V_{eg} is large, $V_{eg} \gg |V_{gg}|, V'_{eg}, t$ [34], neglect mixing of the above sectors, and project the Hamiltonian (5) onto the subspace (6). Using the relations ${}_i \langle l | e_{in}^\dagger e_{im} | p \rangle_i = {}_i \langle l | g_{in}^\dagger g_{im} | p \rangle_i = \frac{1}{2} (\delta_{lp} \delta_{nm} - \delta_{ml} \delta_{np})$, and the pseudo-fermions (4), we obtain an effective model

$$H_{\text{ef}}^A = \sum_{kl} \epsilon_k c_{kl}^\dagger c_{kl} - \sum_i \left[V f_{il}^\dagger f_{ip} c_{il}^\dagger c_{ip} - \frac{U_{gg}}{2} n_i^c (n_i^c - 1) \right] \quad (7)$$

with $V = \frac{V'_{eg} + V_{gg}}{2}$. If the states (6) are identified with VB singlets (2) on a triangle [Fig. 1(e)] by assigning a nuclear spin flavor m to each vertex, H_{ef}^A in 1D is equivalent to (spin-polarized) H_{ef}^{TTLL} in Eq. (3) with $V_{\perp} = V_{\parallel} = V$ [35] plus a Hubbard term, whose role as well as possible ways to introduce anisotropic couplings in Eq. (7) we discuss below. To reach a Kondo screened GS one must have $V > 0$, i.e. $V'_{eg} > -V_{gg} > 0$ [36].

Discussion. Our theory highlights the fundamental role played by the orbital degrees of freedom in stabilizing a *Kondo-screened phase* in the presence of *extreme strong frustration* when only *singlet* local states participate in the low-energy physics, by allowing the conduction electrons to dynamically flip the VB singlets [see Fig. 1(b)]. These microscopic processes lead to delocalization of the local VBs and drive the formation of the VB spin liquid with HF quasiparticles. We illustrated this mechanism by studying a periodic Anderson model on a frustrated triangular tube, and proposed an optical lattice setup to realize this toy model with $SU(3)$ -symmetric AEAs that employ their nuclear-spin degrees of freedom to implement geometrically frustrated plaquettes (e.g. triangles).

Compared to the electronic KL (3), the low-energy model for AEAs (7) has several peculiarities. First, there is the Hubbard term U_{gg} which below half-filling enhances phases with non-zero $SU(3)$ magnetization in Fig. 3(b). However, its magnitude is effectively damped by the density prefactor $\sim (n^c)^2$. We checked that even when $n^c = 0.8$, one needs $U_{gg} > V$ to suppress the Kondo-screened state. Hence this term is unimportant for the Kondo physics. Second, the Hamiltonian H_{ef}^A has full $SU(3)$ symmetry (i.e. $V_{\perp} = V_{\parallel}$) that originates from the symmetry of Eq. (5) and prohibits experimental exploration of the phase diagram in Fig. 3. This symmetry can be broken by a weak external magnetic field B which to the lowest order amounts to replacing

$V_{\perp} \rightarrow V_{\perp} + \frac{V_{gg} - V'_{eg}}{V_{eg}} (\mu_e - \mu_g) B$ ($\mu_{e,g}$ are magnetic moments for e and g atoms). Also, one might use alternative implementations of the $SU(3)$ Kondo effect, e.g. using orbital degrees of freedom [37], instead of the AEAs setup discussed here.

The HF phase in Figs. 2 and 3 can be detected in cold-atom experiments using slow quantum dynamics or time-of-flight measurements [38–40]. The KL model in Eq. (7) can be implemented beyond 1D, which enables us to use AEAs as controlled [because of the $SU(N)$ symmetry] quantum simulators for more complex frustrated Kondo lattices. Although the currently available isotopes ^{87}Sr and ^{173}Yb are believed to have negative exchange couplings V [16–18], we expect that our results summarized in Figs. 2 and 3 can be realized with other AEAs.

Acknowledgments. We are grateful to Gia-Wei Chern and Michael Hermele for illuminating discussions. This work was supported by the NSF (PIF-1211914 and PFC-1125844), AFOSR, AFOSR-MURI, NIST and ARO individual investigator awards.

-
- [1] H. Diep, *Frustrated Spin Systems* (World Scientific Publishing Company, Incorporated, 2004).
- [2] C. Lacroix, P. Mendels, and F. Mila, *Introduction to Frustrated Magnetism: Materials, Experiments, Theory*, Springer Series in Solid-State Sciences (Springer Berlin Heidelberg, 2011).
- [3] H.-Y. Kee and S. Julian, *Physics in Canada* **68**, 95 (2012).
- [4] A. C. Hewson, *The Kondo Problem to Heavy Fermions* (Cambridge University Press, 1997).
- [5] P. Coleman, *Handbook of Magnetism and Advanced Magnetic Materials*, Vol. 1, H. Kronmüller and S. Parkin (eds.) (2007).
- [6] M. S. Kim and M. C. Aronson, *Phys. Rev. Lett.* **110**, 017201 (2013).
- [7] P. Coleman and A. Nevidomskyy, *Journal of Low Temperature Physics* **161**, 182 (2010).
- [8] Q. Si and S. Paschen, *Physica status solidi (b)* **250**, 425 (2013).
- [9] J. H. Pixley, R. Yu, and Q. Si, *Phys. Rev. Lett.* **113**, 176402 (2014).
- [10] B. H. Bernhard, B. Coqblin, and C. Lacroix, *Phys. Rev. B* **83**, 214427 (2011).
- [11] J. Custers, K.-A. Lorenzer, M. Müller, A. Prokofiev, A. Sidorenko, H. Winkler, A. M. Strydom, Y. Shimura, T. Sakakibara, R. Yu, Q. Si, and S. Paschen, *Nat. Mater.* **11**, 189.
- [12] M. N. Kiselev, *International Journal of Modern Physics B* **20**, 381 (2006).
- [13] L. Isaev, K. Aoyama, I. Paul, and I. Vekhter, *Phys. Rev. Lett.* **111**, 157202 (2013).
- [14] P. W. Anderson, in *Frontiers and borderlines in many-particle physics*, edited by R. Broglia and J. Schrieffer (North-Holland, Amsterdam, 1988).
- [15] A. V. Gorshkov, M. Hermele, V. Gurarie, C. Xu, P. S. Julienne, J. Ye, P. Zoller, E. Demler, M. D. Lukin, and A. M. Rey, *Nat. Phys.* **6**, 289 (2010).
- [16] X. Zhang, M. Bishof, S. L. Bromley, C. V. Kraus, M. S. Safronova, P. Zoller, A. M. Rey, and J. Ye, *Science* **345**, 1467 (2014).
- [17] G. Cappellini, M. Mancini, G. Pagano, P. Lombardi, L. Livi, M. Siciliani de Cumis, P. Cancio, M. Pizzocaro, D. Calonico, F. Levi, C. Sias, J. Catani, M. Inguscio, and L. Fallani, *Phys. Rev. Lett.* **113**, 120402 (2014).
- [18] F. Scazza, C. Hofrichter, M. Höfer, P. C. De Groot, I. Bloch, and S. Fölling, *Nat. Phys.* **10**, 779.
- [19] H. Katori, M. Takamoto, V. G. Pal'chikov, and V. D. Ovsinnikov, *Phys. Rev. Lett.* **91**, 173005 (2003).
- [20] L. Balents, *Nature* **464**, 199 (2010).
- [21] B. Mühlischlegel, *Zeitschrift für Physik* **208**, 94 (1968); see also the Supplementary material.
- [22] D. L. Cox and A. Zawadowski, *Exotic Kondo Effects in Metals: Magnetic Ions in a Crystalline Electric Field and Tunneling Centres* (Taylor & Francis, 1999).
- [23] τ_a^b are conjugate generators (note the order of indices a and b). For more details see: A. Auerbach, *Interacting Electrons and Quantum Magnetism*, Graduate Texts in Contemporary Physics (Springer New York, 1994).
- [24] G. Bir and G. Pikus, *Symmetry and Strain-Induced Effects in Semiconductors* (John Wiley and Sons, 1974).
- [25] S. Viola Kusminskiy, K. S. D. Beach, A. H. Castro Neto, and D. K. Campbell, *Phys. Rev. B* **77**, 094419 (2008).
- [26] See the Supplementary material.
- [27] K. Okunishi, M. Sato, T. Sakai, K. Okamoto, and C. Itoi, *Phys. Rev. B* **85**, 054416 (2012).
- [28] K. Seki and K. Okunishi, arXiv:1502.06702.
- [29] Our notion of chirality is similar to the vector chirality in spin systems $\kappa \sim [\mathbf{S}_1 \times \mathbf{S}_2]$ [27]. Indeed, for a given triangle, one can introduce an analogous quantity $\kappa_a = i \sum_{b'c'} \varepsilon_{ab'c'} f_{b'}^\dagger c_{b'}^\dagger c_b f_b$.
- [30] P. Coleman and N. Andrei, *Journal of Physics: Condensed Matter* **1**, 4057 (1989).
- [31] T. Senthil, M. Vojta, and S. Sachdev, *Phys. Rev. B* **69**, 035111 (2004).
- [32] See the Supplementary material.
- [33] Because the s -wave scattering length is $a_{gg} > 0$ [15], two-atom collisions favor antisymmetric spatial wavefunction and symmetric nuclear spin configurations.
- [34] V_{eg} is at least twice larger than V'_{eg} and $|V_{gg}|$ because of the Bloch-function overlap between lowest and excited bands. This overlap can be further decreased by placing itinerant g atoms in higher bands.
- [35] In the case of AEAs, C_{3v} operations should be applied to the nuclear spin states: C_3 rotations perform a cyclic permutation $10\bar{1} \rightarrow \bar{1}10$, the three mirror planes interchange any two states while preserving the third, e.g. $10\bar{1} \rightarrow \bar{1}01$.
- [36] See the renormalization group analysis in the Supplementary Material.
- [37] Y. Nishida, *Phys. Rev. Lett.* **111**, 135301 (2013).
- [38] M. Foss-Feig, M. Hermele, and A. M. Rey, *Phys. Rev. A* **81**, 051603 (2010).
- [39] M. Foss-Feig, M. Hermele, V. Gurarie, and A. M. Rey, *Phys. Rev. A* **82**, 053624 (2010).
- [40] B. Paredes, C. Tejedor, and J. I. Cirac, *Phys. Rev. A* **71**, 063608 (2005).

Supplementary material for: Heavy-fermion valence-bond liquids in ultracold atoms: cooperation of Kondo effect and geometric frustration

$SU(3)$ KL MODEL ON A TTL

In this section we outline a derivation of the KL Hamiltonian (3). We start by considering an Anderson impurity model for an isolated triangle in Fig. 1(a), i.e. a single-rung case of Eq. (1). In the limit of weak valence fluctuations, we use a Schrieffer-Wolff transformation to obtain a second-order Kondo-like impurity Hamiltonian. Because the periodic Anderson model (1) is additive w.r.t. triangular rungs, this Kondo impurity model can be straightforwardly generalized for a periodic array of the “impurities” (triangles), i.e. a TTL.

The single-triangle Anderson impurity model describes three conduction bands coupled to a triangular plaquette

$$\begin{aligned} H_{AIM} &= H_0 + H_{\text{int}} + H_d; \\ H_0 &= \sum_{k\alpha\sigma} \varepsilon_{k\sigma} c_{k\alpha\sigma}^\dagger c_{k\alpha\sigma}; \\ H_{\text{int}} &= \frac{v}{\sqrt{N}} \sum_{k\alpha\sigma} (c_{k\alpha\sigma}^\dagger d_{a\sigma} + \text{h.c.}); \\ H_d &= J_H \mathbf{S}_d^2 - \epsilon_d N_d + U \sum_{a \neq b} n_a^d n_b^d, \end{aligned} \quad (\text{S1})$$

where we used the same notations as in Eq. (1) but omitted the triangle position $x_i = i$. N is the dimensionless system size, e.g. the number of unit cells.

The last line in Eq. (S1) is the Hamiltonian of an isolated triangle. Due to the strong on-site Coulomb repulsion we can treat $d_{a\sigma}$ as constrained fermions (no double occupancy) with anticommutation relations [1]

$$\begin{aligned} \{d_{a\alpha}, d_{b\beta}\} &= \{d_{a\alpha}^\dagger, d_{b\beta}^\dagger\} = 0; \\ \{d_{a\alpha}, d_{b\beta}^\dagger\} &= \delta_{ab} [d_{a\beta}^\dagger d_{a\alpha} + \delta_{\alpha\beta} (1 - n_a^d)], \end{aligned}$$

and consider only three states per vertex a . There are

hence $4^3 = 64$ electronic states. The corresponding energies $E_d(N_d, S_d)$,

$$\begin{aligned} E_d(1, 1/2) &= -\epsilon_d + \frac{3}{4} J_H, \\ E_d(2, 0) &= -2\epsilon_d + U, \\ E_d(2, 1) &= -2\epsilon_d + U + 2J_H, \\ E_d(3, 1/2) &= -3\epsilon_d + 3U + \frac{3}{4} J_H, \\ E_d(3, 3/2) &= -3\epsilon_d + 3U + \frac{15}{4} J_H, \end{aligned}$$

are plotted in Fig. S1. For us the most interest has the two-electron subspace with a singlet GS. This state is three-fold degenerate and corresponds to a global energy minimum for $U - \frac{3}{4} J_H < \epsilon_d < 2U + \frac{3}{4} J_H$. The three singlet ground states are given in Eq. (2).

In the strong-coupling regime $v \ll \epsilon_d, U$ we can use a Schrieffer-Wolff transformation $H = e^{\mathcal{S}} H_{AIM} e^{-\mathcal{S}}$ [2] which is constructed to eliminate H_{int} in each order in v . To the second order we have

$$H_2 = H_0 + H_d + \frac{1}{2} [\mathcal{S}, H_{\text{int}}].$$

The generator \mathcal{S} satisfies the equation $[H_d + H_0, \mathcal{S}] = H_{\text{int}}$ and has the form [3, 4]:

$$\mathcal{S} = \frac{v}{\sqrt{N}} \sum \frac{1}{E'_d - E_d} c_{k\alpha\sigma}^\dagger P'_d d_{a\sigma} P_d - \text{h.c.}$$

Here the summation is over all variable not present in the l.h.s. The operators P_d are projectors on the triangle states with energy E_d , and we neglected the electron bandwidth in the energy denominators.

The matrix elements of the commutator in H_2 can be computed as

$$\begin{aligned} \langle a_1 | [\mathcal{S}, H_{\text{int}}] | a_2 \rangle &= \frac{v^2}{N} \sum \frac{1}{E'_d - E_d} \langle a_1 | (c_{k\alpha\sigma}^\dagger P'_d d_{a\sigma} P_d) (d_{b\beta}^\dagger c_{pb\beta}) - (d_{b\beta}^\dagger c_{pb\beta}) (c_{k\alpha\sigma}^\dagger P'_d d_{a\sigma} P_d) | a_2 \rangle + \text{h.c.} = \\ &= \frac{v^2}{N} \sum \left[\frac{1}{E_d(2, 0) - E_d(3, 1/2)} c_{k\alpha\sigma}^\dagger c_{pb\beta} \langle a_1 | d_{a\alpha} d_{b\beta}^\dagger | a_2 \rangle - \frac{1}{E_d(1, 1/2) - E_d(2, 0)} c_{pb\beta} c_{k\alpha\sigma}^\dagger \langle a_1 | d_{b\beta}^\dagger d_{a\alpha} | a_2 \rangle \right] + \text{h.c.}, \end{aligned}$$

where $E_d(2, 0) - E_d(3, 1/2) = -(2U - \epsilon_d + \frac{3}{4} J_H)$ and $E_d(1, 1/2) - E_d(2, 0) = \epsilon_d - U + \frac{3}{4} J_H$. We will focus on a special case $\epsilon_d = \frac{3}{2} U$ when $E_d(3, 1/2) - E_d(2, 0) = E_d(1, 1/2) - E_d(2, 0) = \Delta$.

Since the states $|a_{1,2}\rangle$ in Eq. (2) are singlets, the matrix elements $\langle a_1 | \dots | a_2 \rangle$ satisfy the property

$$\langle a_1 | d_{a\alpha} d_{b\beta}^\dagger | a_2 \rangle = \delta_{\alpha\beta} \langle a_1 | d_{a\uparrow} d_{b\uparrow}^\dagger | a_2 \rangle = \delta_{\alpha\beta} \langle a_1 | d_{a\downarrow} d_{b\downarrow}^\dagger | a_2 \rangle$$

and similarly for $\langle a_1 | d_{b\beta}^\dagger d_{a\alpha} | a_2 \rangle$. The spin-polarized elements are given by

$$\begin{aligned} \langle a_1 | d_{a\uparrow} d_{b\uparrow}^\dagger | a_2 \rangle &= \delta_{ab} \delta_{a_1 a_2} \delta_{a_2 a} - \frac{1}{2} \delta_{a_1 a} \delta_{a_2 b} (1 - \delta_{ab}), \\ \langle a_1 | d_{b\uparrow}^\dagger d_{a\downarrow} | a_2 \rangle &= \frac{1}{2} \left[\delta_{ab} \delta_{a_1 a_2} (1 - \delta_{a_2 a}) + (1 - \delta_{ab}) \delta_{a_1 a} \delta_{a_2 b} \right]. \end{aligned}$$

Using these expressions and neglecting the constant term that arises from $c_{pb\beta} c_{ka\alpha}^\dagger = \delta_{ab} \delta_{kp} \delta_{\alpha\beta} - c_{ka\alpha}^\dagger c_{pb\beta}$, we arrive at the Kondo impurity model

$$\begin{aligned} H_{\text{ef}} &= \sum_k \epsilon_{k\sigma} c_{ka\sigma}^\dagger c_{ka\sigma} - \frac{V_\perp}{N} \sum_{kp}' f_a^\dagger f_a c_{ka'\sigma}^\dagger c_{pa\sigma} - \\ &\quad - \frac{V_\parallel}{N} \sum_{kp} f_a^\dagger f_a c_{ka\sigma}^\dagger c_{pa\sigma} \end{aligned}$$

with $V_\parallel = \frac{3v^2}{2\Delta}$ and $V_\perp = -\frac{v^2}{2\Delta}$, from which Eq. (3) is recovered by adding a triangle position i , and replacing in the last two terms the summation over k and p with that over i :

$$\frac{1}{N} \sum_{kp} c_{ka'\sigma}^\dagger c_{pa\sigma} \rightarrow \sum_i c_{ia'\sigma}^\dagger c_{ia\sigma}.$$

Note the term H_d gives only a constant energy shift, since $\langle a_1 | H_d | a_2 \rangle = E_d(2, 0) \delta_{a_1 a_2}$, and therefore was dropped. The Hamiltonian H_{ef} can be reduced to a single-channel form using the same arguments as in the main text. Hence, in the following we will consider its spin-polarized version, omit the spin index σ and replace $\epsilon_{k\sigma} \rightarrow \epsilon_k$:

$$H_{\text{ef}} \rightarrow \sum_k \epsilon_k c_{ka}^\dagger c_{ka} - \frac{1}{N} \sum_{kp} V_{ab} f_a^\dagger f_b c_{ka}^\dagger c_{pb} \quad (\text{S2})$$

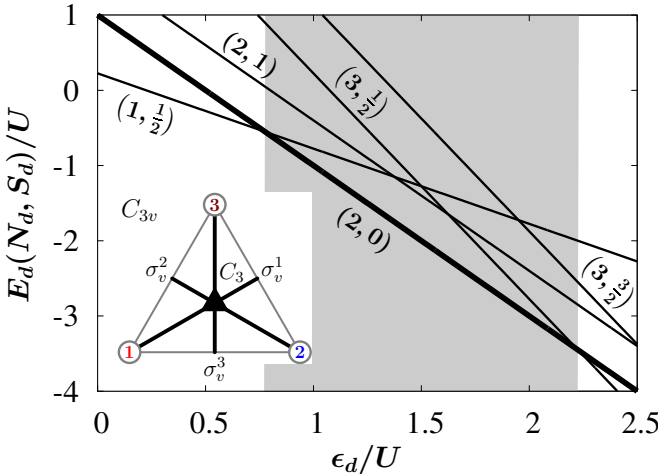


FIG. S1. Energy levels of an isolated triangle. N_d and S_d are the total particle number and spin. In the shaded region the GS has $N_d = 2$ electrons (thick line). Inset: The C_{3v} symmetry group of the triangle, which contains the three-fold axis C_3 and three mirror planes σ_v . The numbers 1...3 indicate the vertices.

with $V_{ab} = V_\perp(1 - \delta_{ab}) + V_\parallel \delta_{ab}$.

Finally we note that an Anderson model similar to Eq. (S1) was studied in the context of tunneling through triple quantum dots [5, 6], solid-state spin entanglers [7], and Kondo physics in frustrated geometries [8, 9], but to our knowledge has never been generalized to a lattice.

PHYSICAL PROPERTIES OF THE $SU(3)$ KL

In this section we elaborate on the discussion in the main text regarding physical properties of the KL model (3). First, we will consider the limit of a single $SU(3)$ impurity in order to identify parameter regimes relevant for Kondo screening. Based on the obtained intuition, we then generalize the hybridization mean-field approach [10] to handle the $SU(3)$ KL model in Eq. (3).

Poor man scaling for a single impurity

We will apply the perturbative (in V_\parallel and V_\perp) renormalization group (RG), i.e. Anderson's poor man scaling described in Ref. 2 to the Kondo impurity model (S2). For simplicity, we assume that the itinerant band has a constant density of states ρ_0 for $\epsilon \in [-D, D]$. Notice that system is not assumed to be 1D.

The perturbative RG approach is a series of consecutive Schrieffer-Wolff transformations that remove high-energy states near the band edges $[D - \delta D, D]$ and $[-D, -D + \delta D]$ with $\delta D > 0$, $\delta D \ll D$. It is assumed that there are no electrons (holes) in the first (second) interval. We will label states inside (outside) these intervals with momenta q, q' (k, p), etc.

The impurity model (S2) can be cast in the form

$$\begin{aligned} H_{\text{ef}} &= \sum_k \epsilon_k c_{ka}^\dagger c_{ka} + \sum_q \epsilon_q c_{qa}^\dagger c_{qa} - \\ &\quad - \frac{1}{N} \sum_{kp} V_{ab} f_b^\dagger f_a c_{kb}^\dagger c_{pa} - \frac{1}{N} \sum_{q'q} V_{ab} f_b^\dagger f_a c_{q'b}^\dagger c_{qa} - \\ &\quad - \frac{1}{N} \sum_{pq} V_{ab} f_b^\dagger f_a (c_{pb}^\dagger c_{qa} + c_{qa}^\dagger c_{pb}), \end{aligned}$$

where the first two lines contain diagonal terms and the last line is an off-diagonal operator $H_1 = -\frac{1}{N} \sum_{pq} V_{ab} f_b^\dagger f_a (c_{pb}^\dagger c_{qa} + c_{qa}^\dagger c_{pb})$ that transfers electrons to and from near the band edges. Note that $H_1 \sim \delta D$ because of the q -summation, and we can neglect the term with $\sum_{q'q} (\dots) \sim (\delta D)^2$. The ‘‘unperturbed’’ Hamiltonian for the band edges can be taken simply as $H_0 = \sum_q \epsilon_q c_{qa}^\dagger c_{qa}$ with $\epsilon_q \approx \pm D$.

The transformation $e^S (H_0 + H_1) e^{-S} \approx H_0 + \frac{1}{2} [S, H_1]$ removes H_1 , and the r.h.s. of this expression provides a correction to the remaining Hamiltonian which now does not contain the band-edge degrees of freedom. All

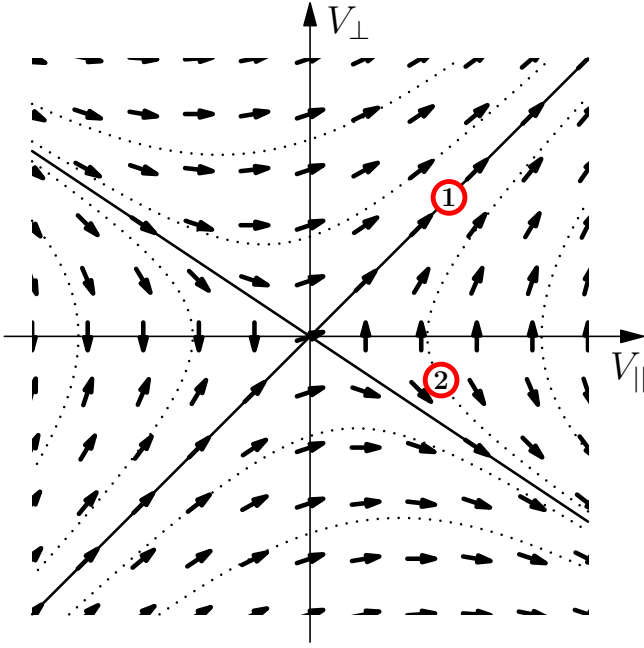


FIG. S2. Renormalization group flow defined by Eq. (S3). Solid lines are the trajectories (S4). Labels 1 and 2 correspond to the two cases studied in the text, and represent the model (S2) with $V_{\perp} = V_{\parallel}$ and $V_{\perp} = -\frac{2}{3}V_{\parallel}$ respectively.

coupling constants in this new Hamiltonian are defined at an energy scale $D - \delta D$. The generator \mathcal{S} is determined by the equation $H_1 = [H_0, \mathcal{S}]$ and can be symbolically written as

$$\mathcal{S} = -\frac{1}{N} \sum \frac{V_{ab}}{E'_0 - E_0} f_b^\dagger f_a c_{pb}^\dagger P'_0 c_{qa} P_0 - \text{h.c.}$$

Here E_0 (E'_0) are eigenstates of H_0 , and P_0 (P'_0) corresponding projectors. The summation extends over all relevant variables.

A straightforward calculation of the commutator $[\mathcal{S}, H_1]$ yields the RG equations:

$$\begin{aligned} V_{\perp}(D - \delta D) &= V_{\perp}(D) + V_{\perp}(V_{\perp} + 2V_{\parallel}) \frac{\rho_0 \delta D}{D}, \\ V_{\parallel}(D - \delta D) &= V_{\parallel}(D) + 3V_{\perp}^2 \frac{\rho_0 \delta D}{D}, \end{aligned}$$

or in a differential form:

$$\frac{dV_{\perp}}{d \ln D} = -\rho_0 V_{\perp}(V_{\perp} + V_{\parallel}); \quad \frac{dV_{\parallel}}{d \ln D} = -3\rho_0 V_{\perp}^2. \quad (\text{S3})$$

The flow trajectories (integrals of motion) are obtained by excluding $\ln D$ from these expressions, i.e. $dV_{\parallel}/dV_{\perp} = 3V_{\perp}/(2V_{\parallel} + V_{\perp})$. This is a Darboux equation [11], whose solution is

$$(V_{\perp} - V_{\parallel})^3 \left(V_{\perp} + \frac{2}{3}V_{\parallel} \right)^2 = \text{const.} \quad (\text{S4})$$

It is easy to find the RG flow in two special regimes: (1) $V_{\perp} = V_{\parallel}$ [full $SU(3)$ symmetry] and (2) $V_{\perp} = -\frac{2}{3}V_{\parallel}$, both corresponding to $\text{const} = 0$ in Eq. (S4). Assuming that $V_{\parallel} = V_{\parallel}^{(0)}$ for some fixed value of $D = D_0$, in the first case we have: $V_{\parallel}(D) = V_{\parallel}^{(0)} / [1 - 3\rho_0 V_{\parallel}^{(0)} \ln \frac{D_0}{D}]$. In the second case the solution is $V_{\parallel}(D) = V_{\parallel}^{(0)} / [1 - \frac{4}{3}\rho_0 V_{\parallel}^{(0)} \ln \frac{D_0}{D}]$. Upon reducing the bandwidth $D < D_0$, V_{\parallel} always increases. Hence, for $V_{\parallel}^{(0)} > 0$, the flow is always towards strong coupling indicating a Kondo-screened GS. The scaling trajectories for a general case are shown in Fig. S2.

The hybridization mean-field approach

The RG flow in Fig. S2 suggests that for $V_{\parallel} > 0$, the impurity model (S2) always exhibits the Kondo screening. Similar to the $SU(2)$ case [10], one may expect that the same is true for the lattice model (3). Here we demonstrate this by using a modified slave boson (hybridization) mean-field approach that replaces pseudo-fermions f_{ia} in Eq. (3) with canonical fermions at unit filling:

$$n_i^f = 1 \rightarrow \frac{1}{N} \sum_i \langle n_i^f \rangle = 1, \quad (\text{S5})$$

where $n_i^f = f_{ia}^\dagger f_{ia}$ and N is the number of lattice sites.

The correct slave boson fields can be identified by diagonalizing the interaction part in Eq. (3) on a single site assuming that there is one f - and c -fermion. There are nine eigenstates

$$\begin{aligned} |\psi_0\rangle &= \frac{1}{\sqrt{3}} \sum_a f_{ia}^\dagger c_{ia}^\dagger |\text{vac}\rangle; \\ |\psi_{1,2}\rangle &= \frac{1}{\sqrt{3}} (f_{i1}^\dagger c_{i1}^\dagger + \omega^{\pm 1} f_{i2}^\dagger c_{i2}^\dagger + \omega^{\mp 1} f_{i3}^\dagger c_{i3}^\dagger) |\text{vac}\rangle; \\ |\psi_{3\dots 8}\rangle &= f_{ia}^\dagger c_{ib}^\dagger |\text{vac}\rangle \quad \text{with } a \neq b \end{aligned} \quad (\text{S6})$$

with energies $E_0 = -(V_{\parallel} + 2V_{\perp})$, $E_1 = E_2 = -(V_{\parallel} - V_{\perp})$, $E_{3\dots 8} = 0$, and $\omega = e^{2\pi i/3}$.

The states $|\psi_{1,2}\rangle$ transform according to the two-dimensional representation of the group C_{3v} [12]. The symmetry operations from this group are shown in the inset of Fig. S1, and their matrices in the basis $|\psi_{1,2}\rangle$ are given by:

$$C_3 = \begin{pmatrix} \omega & 0 \\ 0 & \omega^* \end{pmatrix}, \quad \sigma_v^1 = \begin{pmatrix} 0 & 1 \\ 1 & 0 \end{pmatrix}, \quad \sigma_v^2 = \begin{pmatrix} 0 & \omega \\ \omega^* & 0 \end{pmatrix}, \quad \sigma_v^3 = (\sigma_v^2)^*$$

The state $|\psi_0\rangle$ is invariant under all operations from C_{3v} .

Each of the states (S6) can be associated with a Schwinger boson $\hat{\chi}_{in}$ (for a fixed i), and we can formally

write the Kondo term as

$$\begin{aligned} H_K &= \sum_i \Lambda_{ab}^{a'b'} f_{ia'}^\dagger c_{ib'}^\dagger c_{ib} f_{ia} = \\ &= \sum_{in} E_n \langle a'b' | n \rangle \langle n | ab \rangle f_{ia'}^\dagger c_{ib'}^\dagger c_{ib} f_{ia} = \\ &= \sum_{in} E_n \hat{\chi}_{in}^\dagger \hat{\chi}_{in}. \end{aligned}$$

In our case the slave bosons are actually pairing fields:

$$\begin{aligned} \hat{\chi}_{i0} &= \frac{1}{\sqrt{3}} \sum_a f_{ia} c_{ia}; \\ \hat{\chi}_{i1,2} &= \frac{1}{\sqrt{3}} (f_{i1} c_{i1} + \omega^{\mp 1} f_{i2} c_{i2} + \omega^{\pm 1} f_{i3} c_{i3}) \end{aligned} \quad (S7)$$

Other χ_{in} with $n = 3 \dots 8$ do not appear due to vanishing eigenvalues $E_{3\dots 8}$.

We assume that the system is homogeneous so all averages are i -independent, and perform a Hartree-Fock-Bogoliubov decoupling in two ‘‘channels’’: (i) Hybridization channel, by condensing the χ -bosons, i.e. considering the averages $\chi_n = \langle \hat{\chi}_{in} \rangle$, and (ii) magnetization channel, defined by the traceless parts of $\langle f_{ia}^\dagger f_{ib} \rangle$ and $\langle c_{ia}^\dagger c_{ib} \rangle$. The latter can be expanded in terms of Gell-Mann matrices λ^l with $l = 1 \dots 8$:

$$\begin{aligned} \langle f_{ia}^\dagger f_{ib} \rangle &= \sum_l \lambda_{ab}^l m_l^f + \frac{1}{3} \delta_{ab}, \\ \langle c_{ia}^\dagger c_{ib} \rangle &= \sum_l \lambda_{ab}^l m_l^c + \frac{n^c}{3} \delta_{ab}. \end{aligned}$$

Our convention for the Gell-Mann matrices is:

$$\begin{aligned} \lambda^1 &= \begin{pmatrix} 0 & 1 & 0 \\ 1 & 0 & 0 \\ 0 & 0 & 0 \end{pmatrix}, \quad \lambda^2 = \begin{pmatrix} 0 & -i & 0 \\ i & 0 & 0 \\ 0 & 0 & 0 \end{pmatrix}, \quad \lambda^3 = \begin{pmatrix} 1 & 0 & 0 \\ 0 & -1 & 0 \\ 0 & 0 & 0 \end{pmatrix}, \\ \lambda^4 &= \begin{pmatrix} 0 & 0 & 1 \\ 0 & 0 & 0 \\ 1 & 0 & 0 \end{pmatrix}, \quad \lambda^5 = \begin{pmatrix} 0 & 0 & -i \\ 0 & 0 & 0 \\ i & 0 & 0 \end{pmatrix}, \quad \lambda^6 = \begin{pmatrix} 0 & 0 & 0 \\ 0 & 0 & 1 \\ 0 & 1 & 0 \end{pmatrix}, \\ \lambda^7 &= \begin{pmatrix} 0 & 0 & 0 \\ 0 & 0 & -i \\ 0 & i & 0 \end{pmatrix}, \quad \lambda^8 = \frac{1}{\sqrt{3}} \begin{pmatrix} 1 & 0 & 0 \\ 0 & 1 & 0 \\ 0 & 0 & -2 \end{pmatrix}. \end{aligned}$$

The mean-field Hamiltonian has the form:

$$\begin{aligned} H_{\text{MF}} &= \sum_k [(\epsilon_k - \mu_c) \delta_{ab} - M_{ab}^f] c_{ka}^\dagger c_{kb} + \\ &+ \sum_k [\mu_f \delta_{ab} - M_{ab}^c] f_{-ka}^\dagger f_{-kb} - \\ &- \sum_k [V_a c_{ka}^\dagger f_{-ka}^\dagger + V_a^* f_{-ka} c_{ka}] = \\ &= \sum_k (c_{ka}^\dagger \quad f_{-ka}) \mathcal{H}_k \begin{pmatrix} c_{kb} \\ f_{-kb} \end{pmatrix} \end{aligned}$$

with

$$\mathcal{H}_k = \begin{pmatrix} (\epsilon_k - \mu_c) \delta_{ab} - M_{ab}^f & -V_a \delta_{ab} \\ -V_a^* \delta_{ab} & -\mu_f \delta_{ab} + M_{ba}^c \end{pmatrix}.$$

Here summations over color indices are implicit and the k -summation extends over the entire Brillouin zone. The chemical potential μ_f enforces the constraint (S5), while μ_c fixes an average number of the itinerant fermions:

$$\frac{1}{N} \sum_{ka} \langle c_{ka}^\dagger c_{ka} \rangle = n^c.$$

Finally, the mean fields are $M_{ab}^{c,f} = [V_{\parallel} \delta_{ab} + V_{\perp} (1 - \delta_{ab})] \sum_l \lambda_{ab}^l m_l^{c,f}$, and $\sqrt{3} V_a = (V_{\parallel} + 2V_{\perp}) \chi_0 + (V_{\parallel} - V_{\perp}) [\chi_1 \omega + \chi_2 \omega^*]$. The Hamiltonian H_{MF} can be diagonalized by a Bogoliubov transformation [13]

$$\begin{pmatrix} c_{ka} \\ f_{-ka}^\dagger \end{pmatrix} = \sum_s^{n_+(k)} X^s(k) \gamma_{ks} + \sum_t^{n_-(k)} Y^t(k) \beta_{kt}^\dagger$$

with n_+ [n_-] is the number of positive [negative] eigenvalues $E_s(k)$ [$-E_t(k)$] ($E_{s,t} > 0$) of \mathcal{H}_k . These numbers of course depend on k and the mean-field parameters. The fermionic quasiparticles γ_{ks} and β_{kt} define the particle-hole excitations and have only positive energies:

$$H_{\text{MF}} \rightarrow \sum_k \left[\sum_s^{n_+(k)} E_s(k) \gamma_{ks}^\dagger \gamma_{ks} + \sum_t^{n_-(k)} E_t(k) \beta_{kt}^\dagger \beta_{kt} \right].$$

We also note a useful relation

$$\begin{aligned} n^c - n^f &= n^c - 1 = \\ &= \frac{1}{N} \sum_k \left[\sum_s^{n_+(k)} n_{ks}^\gamma - \sum_t^{n_-(k)} n_{kt}^\beta + n_-(k) - 3 \right]. \end{aligned}$$

Once the quasiparticles are known, we can self-consistently determine the order parameters χ_n and $m_l^{c,f}$.

Stability of Kondo-screened phases against lead-mixing perturbations H_{mix}

In the main text we only briefly mentioned effects of the lead-mixing term H_{mix} in Eq. (1) on the heavy-fermion phases in Figs. 2 and 3. Here we provide a more detailed discussion of this issue.

The simplest form of H_{mix} compatible with C_{3v} symmetry of the TTL corresponds to hopping of itinerant and local fermions around a triangle:

$$H_{\text{mix}} = -t_{\Delta}^c \sum_{\langle ab \rangle, k\sigma} c_{ka\sigma}^\dagger c_{kb\sigma} - t_{\Delta}^d \sum_{\langle ab \rangle, i\sigma} d_{ia\sigma}^\dagger d_{ib\sigma} + \text{h.c.},$$

where $t_{\Delta}^{c,d}$ are hopping amplitudes for itinerant and local fermions, and $\langle ab \rangle$ is a triangle edge (nearest-neighbor

link). This Hamiltonian is diagonalized by introducing a transverse momentum $\lambda = 0, \pm \frac{2\pi}{3}$:

$$H_{\text{mix}} = \sum_{k\lambda\sigma} \xi_{\lambda}^c c_{k\lambda\sigma}^{\dagger} c_{k\lambda\sigma} + \sum_{i\lambda\sigma} \xi_{\lambda}^d d_{i\lambda\sigma}^{\dagger} d_{i\lambda\sigma}.$$

with $\xi_{\lambda}^{c,d} = -2t_{\Delta}^{c,d} \cos \lambda$, $c_{k\lambda\sigma} = \frac{1}{\sqrt{3}} \sum_a e^{-i\lambda a} c_{ka\sigma}$ and similarly for $d_{i\lambda\sigma}$. In all other terms in H^{TTL} (1) we can simply replace the lead index a with λ and repeat calculations leading to the KL model (3) using the dressed fermions $c_{k\lambda\sigma}$ and $d_{i\lambda\sigma}$. Note, that the replacement $a \rightarrow \lambda$ also needs to be performed in the expression (2) for the VB singlets. The d -term in H_{mix} is diagonal in the basis of the VB states. For example, $\sum_{\sigma} d_{i\lambda\sigma}^{\dagger} d_{i\lambda\sigma} |1\rangle_i = (\xi_2^d + \xi_3^d) |1\rangle_i = -\xi_1^d |1\rangle_i$ because $\sum_{\lambda} \xi_{\lambda}^{c,d} = 0$, so in general $\sum_{\sigma} d_{i\lambda\sigma}^{\dagger} d_{i\lambda\sigma} |a\rangle_i = -\xi_a^d |a\rangle_i$. Hence, the net effect of H_{mix} amounts to introducing Zeeman splittings $h_{\lambda}^c = \xi_{\lambda}^c$ for c -fermions and $h_{\lambda}^d = -\xi_{\lambda}^d$ for the local $SU(3)$ spins:

$$\delta H_{\text{ef}}^{TTL} = \sum_{i\lambda} (h_{\lambda}^c c_{i\lambda}^{\dagger} c_{i\lambda} + h_{\lambda}^d f_{i\lambda}^{\dagger} f_{i\lambda}).$$

In the context of the $SU(2)$ spin Kondo physics it is known [2] that a sufficiently large magnetic field (of the order of the Kondo temperature) suppresses the Kondo effect. The same will happen in our case: The lead-mixing hopping amplitudes $t_{\Delta}^{c,d}$ play the role of an applied field, and when they become large enough the local GS degeneracy on each triangular plaquette will be lifted

which in turn will destroy the frustrated heavy-fermion phases in Figs. 2 and 3.

-
- [1] C. D. Batista and G. Ortiz, *Advances in Physics* **53**, 1 (2004).
 - [2] A. C. Hewson, *The Kondo Problem to Heavy Fermions* (Cambridge University Press, 1997).
 - [3] B. Mühlischlegel, *Zeitschrift für Physik* **208**, 94 (1968).
 - [4] L. Isaev, K. Aoyama, I. Paul, and I. Vekhter, *Phys. Rev. Lett.* **111**, 157202 (2013).
 - [5] T. Kuzmenko, K. Kikoin, and Y. Avishai, *Phys. Rev. Lett.* **96**, 046601 (2006).
 - [6] R. López, T. c. v. Rejec, J. Martinek, and R. Žitko, *Phys. Rev. B* **87**, 035135 (2013).
 - [7] D. S. Saraga and D. Loss, *Phys. Rev. Lett.* **90**, 166803 (2003).
 - [8] K. Ingersent, A. W. W. Ludwig, and I. Affleck, *Phys. Rev. Lett.* **95**, 257204 (2005).
 - [9] A. K. Mitchell, T. F. Jarrold, M. R. Galpin, and D. E. Logan, *The Journal of Physical Chemistry B* **117**, 12777 (2013), PMID: 23527540.
 - [10] P. Coleman, *Handbook of Magnetism and Advanced Magnetic Materials*, Vol. 1, H. Kronmüller and S. Parkin (eds.) (2007).
 - [11] V. Zaitsev and A. Polyanin, *Handbook of Exact Solutions for Ordinary Differential Equations* (CRC Press, 2002).
 - [12] G. Bir and G. Pikus, *Symmetry and Strain-Induced Effects in Semiconductors* (John Wiley and Sons, 1974).
 - [13] J. Blaizot and G. Ripka, *Quantum Theory of Finite Systems* (Cambridge, MA, 1986).